

How Fast Can a Sailboat Go?

Alan Kruppa

1 Introduction

At the 65+ knot speeds achieved by modern high-speed sailboats, the hydrodynamic efficiencies of hull elements play the dominant role in top speed performance yet the combined aerodynamic efficiencies of sail and superstructure elements begin to play an increasingly balanced role. It becomes necessary, therefore, to optimize high-speed sailboats for supercavitation hydrodynamically and low parasitic drag aerodynamically. A new design with a patented sail and hull configuration is introduced and shown here to have the best combination of aerodynamic and hydrodynamic efficiencies, maximizing the theoretical boat speed to wind speed ratio achievable when looked at in the context of the Beta Theorem.

From this section onward, a **bold-italics** convention is used to build the **roadmap** connecting the theory to the design. New concepts are introduced in bold and then summarized in numbered statements in italics, which are the essence of the roadmap.

0. *A bold-italics convention is used to build the roadmap connecting theory to design.*

2 Inspiration

Growing up in a landlocked small town, I was never exposed to sailing but was always fascinated with it. And when it came time to pick a college, this fascination might have had something to do with my selection of the Naval Academy, especially considering the information booklet about the school had a cover photo of students sailing on one of the Academy's 44 foot sloops, which the booklet explained was one of twenty *Navy 44* sailboats used in training and offshore races. Needless to say, I took up skipper training almost immediately after beginning my first year there in the fall of 2000, waking up early each Saturday morning to study boat systems and practice seamanship on the Severn River and Chesapeake Bay. I spent a fair amount of time at the library as well, often in the periodicals section, and that was where I ran across an article in the January 2001 issue of *Popular Science* magazine about *The*

Race, a no-rules, no-limits, round-the-world sailboat race set to begin on December 31, 2000 [1].

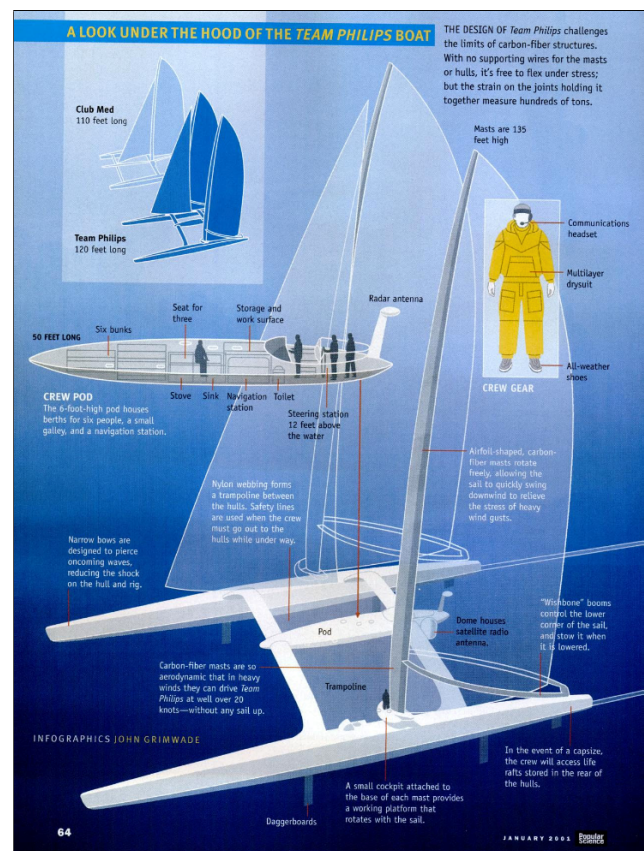


Figure 1: My inspiration for this endeavor: the *Team Philips* catamaran as taken from the January 2001 issue of *Popular Science*

One boat purpose-built for this event, the *Team Philips* catamaran skippered by Pete Goss and shown in Figure 1, was the most extreme and beautiful of the fleet. Each 120 foot wave-piercing hull supported a 135 foot free-standing mast. Suspended between the hulls 12 feet off the water was an aerodynamic center pod and steering station. The view forward was unobstructed and, I can only imagine, exhilarating at the 40+ knot speeds it was capable of. This was like nothing I had ever encountered in my limited sailing experience, and it was not until much later that I realized how much this boat inspired me.

Over the next couple of years, I was fortunate to crew on Naval Academy boats in the Marion Bermuda and Newport Bermuda races. And in the meantime I had earned my skipper qualification. But around this same time, there was an unfortunate policy change revoking the privilege of qualified students to skipper the *Navy 44s*. This was, admittedly, quite disheartening so I decided to take a break from sailing, the timing of which would turn out to be quite serendipitous.

Some 2 years later, I graduated with a degree in aerospace engineering and soon thereafter earned a Masters in the same from the University of Maryland. It was during my Navy service a few years later that I came across yet another sailing article, this time about Ellen MacArthur. I saw a photo of her sailing the B&Q trimaran in which she set the singlehanded round-the-world sailing record, and something just grabbed me about it. I was close enough to my education yet distant enough from sailing—thanks to that serendipitous break—to look at this boat with a critical yet optimistic eye. I found myself looking for ways to reduce drag on the sails and the superstructure and began to sketch out novel concepts along these lines every night at home.

3 Insight

3.1 The Fundamental Question

But beyond just improving this state-of-the-art B&Q trimaran, I started wondering what limits any sailboat’s speed, which led me to the fundamental question: **How fast can a sailboat go?** I started researching sailing speed records and came across a then recent article from the October 2005 issue of *Popular Science* magazine. The title was “The Race to 50 Knots”, and it was about four exotic looking sailboats from around the world trying to break the world sailing speed record, namely the 500 m [or outright] record, which was held then by a windsurfer and was just shy of 50 knots [2].

1. This is the fundamental question: How fast can a sailboat go?

3.2 Aero-Hydrodynamics

Wait a second, windsurfers? Those aren’t boats... No disrespect to windsurfers, obviously, but there was, in fact, something seemingly paradoxical about this, namely a full size boat should have a power advantage over such a small craft, right? But then I remembered back to a little diagram in the *Annapolis Book of Seamanship* that I had come across during my skipper training some 5 years earlier: a rear view free body diagram of a windsurfer with the aerodynamic lift vector pointing diagonally upward, partially lifting

the windsurfer out of the water. The diagram was illustrating how, by using aerodynamic lift and positioning the ballast—in this case, the surfer—above the waterline, a windsurfer greatly reduces hydrodynamic drag while still preventing the craft from heeling over [3].

What this means, then, is that the aerodynamics and hydrodynamics—or **aero-hydrodynamics**, to borrow from C. A. Marchaj’s *Aero-Hydrodynamics of Sailing* [4]—of a sailboat **are coupled [or interdependent] because of the necessity for a mechanism to balance the heeling moment**. In order to remain balanced, a sailboat must always employ a coupled set of aerodynamic and hydrodynamic—again, aero-hydrodynamic—forces, not to mention gravity. So even though windsurfers are smaller and less powerful, they more than make up for it with a balancing mechanism designed for speed.

2. A sailboat’s aero-hydrodynamics are coupled by the mechanism used to balance the heeling moment.

3.3 Glide Angles

In addition to aero-hydrodynamic coupling, I recognized the similarity between aptly named sailplanes, or gliders, and sailboats. Both gliders and sailboats are driven forward by opposing forces: the aerodynamic force and gravity on a glider; the opposing aerodynamic and hydrodynamic forces on a sailboat.

And in the case of a glider, which is shown in Figure 2, performance (e.g. time aloft, maneuverability) is primarily dependent on a low **glide angle (ϵ)**, implying that a glider is—in common parlance—very *aerodynamic*. But technically speaking, a low glide angle corresponds to a high glide ratio (L/D), where the lift (L) and drag (D) forces are defined as the forces perpendicular and parallel to the freestream air velocity (V_∞), respectively. They are related to (ϵ) by a trigonometric relationship:

$$\cot \epsilon = \frac{L}{D} \quad (1)$$

So I knew that in some way a sailboat’s performance—boat speed, specifically—must also depend on its glide angles. **But instead of just one glide angle ϵ , a sailboat has two: the aerodynamic glide angle (ϵ_A) and the hydrodynamic glide angle (ϵ_H)**. And as an aerospace engineering graduate, I recognized that even those four exotic looking sailboats covered in “The Race to 50 Knots” were all lacking in this way; they were all aerodynamically inefficient (i.e. their aerodynamic glide angles were larger than necessary) when compared to most aircraft, especially gliders.

3. Boat speed depends on a sailboat’s aerodynamic and hydrodynamic glide angles ϵ_A and ϵ_H .

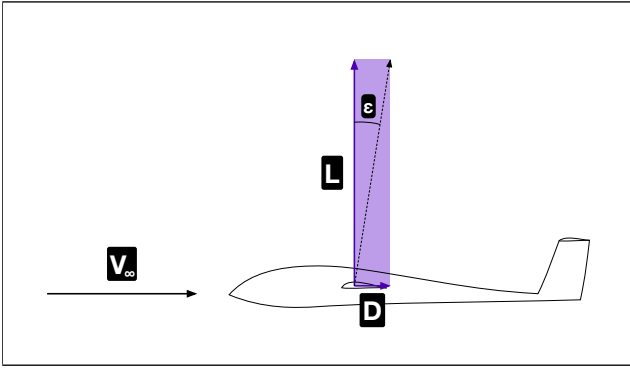


Figure 2: A sailplane, or glider, illustrating the relationship between a glide angle (ϵ) and the lift (L) and drag (D) components

Before continuing, it is worth noting that we typically look at a glider in a gliding mode, where its nose is pointing slightly downward indicating descent. For completeness, this mode is illustrated explicitly in Figure 3, where W is the weight of the glider and F_A is the aerodynamic resultant force, which is the vector sum of the lift and drag vectors. The glide angle ϵ is named as such because it matches the descent angle of an aircraft in a gliding mode.

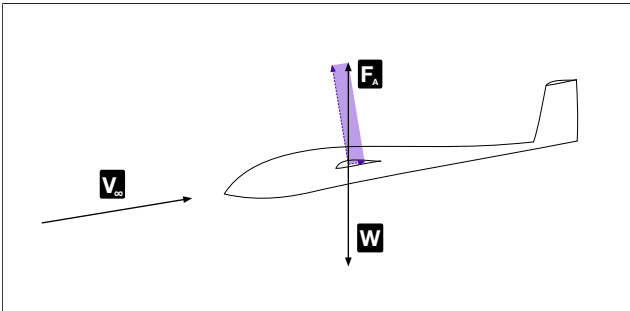


Figure 3: Modified version of Figure 2 showing the glider in a gliding, or descending, mode, where the weight vector (W) and aerodynamic resultant force vector (F_A) are in balance

3.4 Top Speed & Efficiency

So now that we know about coupling and glide angles, we can go back a bit and approach the question posed in (1) by introducing two intuitive assumptions about hypothetical sailboats named A and B: 1. If A and B are identical, but A is sailing in higher true winds than B, A will sail faster than B; and 2. If A and B are not identical, such that A can sail at a higher boat speed to true wind speed ratio, then if A is sailing in identical true winds to B, A will sail faster than B. What these two assumptions are really saying is that a sailboat's speed is dependent on both true wind speed and **efficiency** (η), defined as the ratio of boat speed (V_H) to true wind speed (V_T):

$$\eta = \frac{V_H}{V_T} \quad (2)$$

As obvious as these assumptions may seem, this formal distinction between that part of a boat's speed affected by wind and that part affected by efficiency is crucial to establishing the framework for comparing and optimizing sailboat designs for speed because only efficiency applies to the boat itself. So this means that in order to compare the **top speed potentials** of sailboats, we need only compare their efficiencies. In practice, efficiency as defined in Equation 2 is not entirely independent from the true wind velocity (i.e. speed and direction) so for now we will assume a port (i.e. left when looking at the bow) tack beam reach, which means that the wind is coming from the **9 o'clock position**. We will return to the topic of the wind direction dependency later in Section 4.1.5 when talking about the fastest point of sail.

4. Boat speed increases with true wind speed (V_T) and efficiency (η), but we only use efficiencies for comparing top speed potentials. And for now, we are assuming that the wind is coming from the 9 o'clock position.

3.5 The Ideal Sailboat

We have reasonably decided to use efficiency to compare top speed potentials, but from a design point of view, we want to be able to compare top speed potentials of concepts, not actual boats. So we need a way to calculate a sailboat's efficiency without actually sailing and measuring it. In order to do this, we need to figure out how to relate efficiency to a sailboat's two glide angles, which are predictable characteristics of the boat itself, knowing only that the true wind direction is assumed to be at the 9 o'clock position. The simplest starting point for the study of efficiency is an **ideal sailboat**, which is shown in Figure 4 and which has no heeling moment, zero mass, and comprises only two parts: a vertical aerodynamic wing above the waterline plane connected along a pivoting axis to a vertical hydrodynamic foil below the waterline plane.

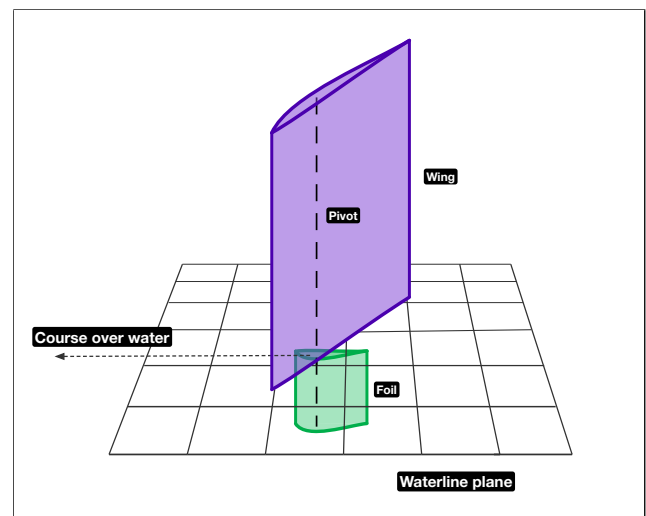


Figure 4: An ideal sailboat comprising a vertical wing and a vertical foil, attached along a pivoting axis

By removing heeling from the problem, we eliminate aero-hydrodynamic coupling. And because both the wing and the foil are vertical, the forces on an ideal sailboat can be analyzed in just two dimensions rather than three. Finally, because it has no mass, it has no lost lift, which we will cover later in Section 3.6.3. In other words, the efficiency of an ideal sailboat must be—as we will show—solely dependent on the glide angles of the wing above the waterline plane in the aerodynamic domain and the foil below the waterline plane in the hydrodynamic domain.

If we isolate the wing of this ideal sailboat in a top view free body diagram as shown in Figure 5, the similarity between it and the glider shown in Figure 2 is readily apparent, where V_A , L_A , D_A , and ε_A are direct analogues to V_∞ , L , D , and ε . Beyond that, we have explicitly labeled the dashed arrow representing the aerodynamic resultant force vector (F_A), which is the net force *felt* by the wing and which we mentioned earlier is the vector sum of L_A and D_A . The apparent wind angle β shown is defined as the angle between the apparent wind velocity (V_A) and the hydrodynamic velocity (V_H), the latter having a magnitude equal to the boat speed and a direction opposite to the course over water.

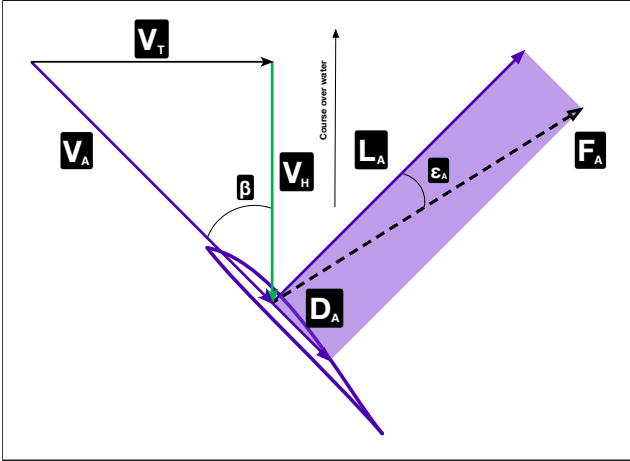


Figure 5: **Top view free body diagram of the wing on an ideal sailboat**

It is worth taking a step back here to remind ourselves of why we are looking at these free body diagrams: we want to relate efficiency to glide angles. And it turns out that there are two insights needed to do this. The first of these insights, which we can draw from Figure 5, is that V_H and V_T form a right triangle with β when the true wind velocity (V_T) is blowing from the 9 o'clock position. So the three are related by a trigonometric relationship:

$$\cot \beta = \frac{V_H}{V_T} \quad (3)$$

And because we earlier defined efficiency with the expression $\eta = V_H/V_T$, we can then say that

$$\eta = \cot \beta \quad (4)$$

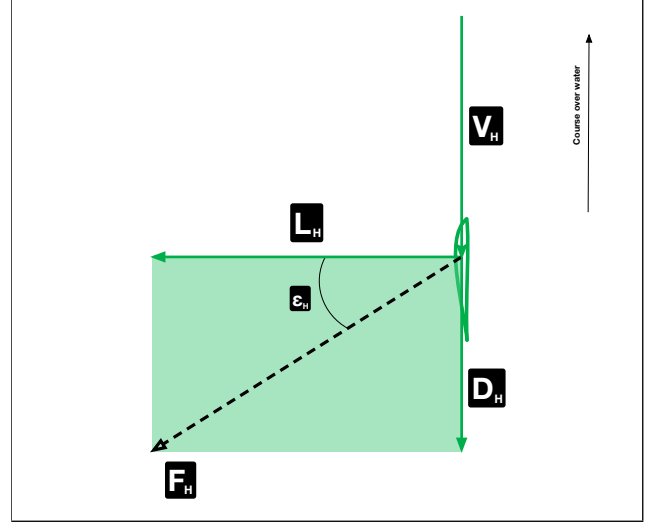


Figure 6: **Top view free body diagram of the foil on an ideal sailboat**

For completeness before going forward, let us now isolate the foil in a top view free body diagram as shown in Figure 6, similar to the way in which we isolated the wing in Figure 5. Again, the similarity to the glider in Figure 2 is readily apparent. Only this time, V_H , L_H , D_H , and ε_H are direct analogues to V_∞ , L , D , and ε . And again, we have explicitly labeled the dashed line representing the hydrodynamic resultant force vector (F_H).

Combining the wing and foil free body diagrams along the pivoting axis, we get the complete free body diagram of an ideal sailboat shown in Figure 7. The aerodynamic and hydrodynamic resultant force vectors, F_A and F_H , respectively, are equal and opposite. This is a necessary condition at equilibrium.

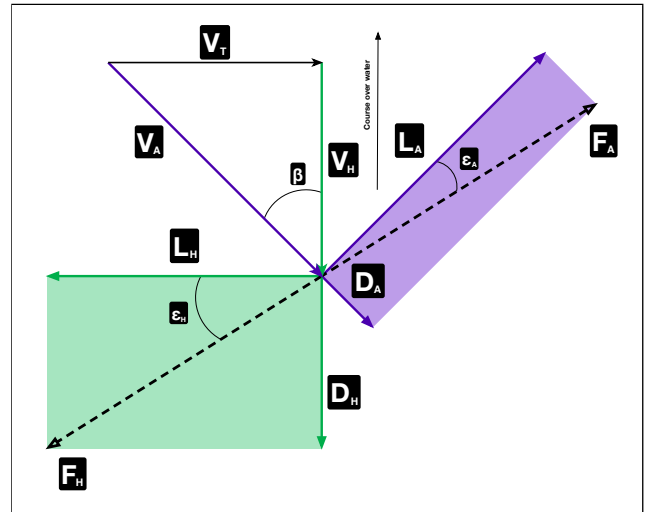


Figure 7: **Top view free body diagram of an ideal sailboat with the wind at the 9 o'clock position**

We are almost there. It turns out that the second key insight necessary to relate efficiency to glide angles is a geometric one, and it concerns the relationship between β , ε_A , and ε_H . By drawing a line perpendicular to the resultant force vectors in Figure 7, we get the modified diagram shown in Figure 8.

We can see that the two angles formed by this line dividing β —this is called the sailing axis for reasons we will discuss later in Section 4.2—are the same as ε_A and ε_H , as shown. As Ross Garrett states in *The Symmetry of Sailing*: “...the [apparent wind] angle β is simply the sum of the sail and hull [glide] angles.” He coins this “deceptively simple” relationship the **Beta Theorem** [5]:

$$\beta = \varepsilon_A + \varepsilon_H \quad (5)$$

Combining this with the trigonometric function for efficiency, $\eta = \cot \beta$, we see that efficiency is related to glide angles in the following way:

$$\eta = \cot(\varepsilon_A + \varepsilon_H) \quad (6)$$

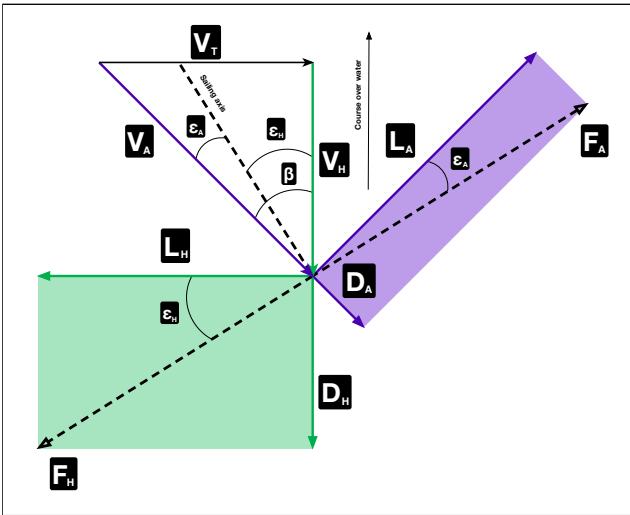


Figure 8: Modified version of Figure 7 illustrating the relationship between β , ε_A , and ε_H

Remember, we assumed a 9 o'clock wind position. The expression above becomes a little more complicated when other wind directions are used, and we will revisit this expression later when talking about the fastest point of sail in Section 4.1.5. But even after revisiting it later, it will become apparent to you that this simpler expression will still be the one we use for comparing top speed potentials regardless of the wind direction!

5. Efficiency is related to the glide angles by the expression $\eta = \cot(\varepsilon_A + \varepsilon_H)$, which we found by using the Beta Theorem while assuming a 9 o'clock wind position.

3.6 Real-World Sailboats

3.6.1 Mechanisms for Balance

So far we have talked about sailboats in purely theoretical terms by introducing the concept of the ideal sailboat, which is completely unrealistic. A real-world sailboat must obviously have some mechanism for balancing the heeling moment. There are three primary ways high-speed sailboats do this: 1. conventional windward ballast like that found on the *Macquarie Innovation* sailboat; 2. force-alignment like that found on the current record holder, *Vestas Sailrocket 2*; and 3. aeroballast like that found on the *Radboat* design introduced here.

These three mechanisms are illustrated in a greatly simplified cartoon-like manner alongside an ideal sailboat in Figure 9. This is how they would look from both the front (i.e. from a point upstream) and the top on a port tack. The legend at the bottom explains what each of the color coded arrows means. In all three cases, we have made six good design assumptions: 1. there is a single foil (i.e. below the waterline) producing useful lift; 2. the only surfaces touching the water are the single foil and the planing surfaces; 3. the number of planing surfaces is minimized; 4. there is a single wing (i.e. above the waterline) producing useful lift; 5. the weight of the boat is supported by the wing for the force-aligned and aeroballast configurations (i.e. there is no weight being supported by the planing surfaces); and 6. superstructure (i.e. above the waterline) is minimized and streamlined.

We have used the same purple and green color coding to represent the wing and foil, respectively, as was used in the top view diagrams of an ideal sailboat presented in Figures 5 through 8. And again, the purple and green arrows represent what we are now calling useful lift. But we have also had to add six new items, which are presented in the legend in Figure 9: 1. lost lift represented by a gray arrow and equal to the amount of lift generated by a wing, plane, or foil beyond what is useful; 2. weight represented by a black arrow and equal to the total physical weight of the boat; 3. crossarm represented by a black line and connecting aerodynamic superstructure; 4. C.G. represented by a checkered circle and indicating the location of the center of gravity; 5. fairing represented by a black-outlined teardrop shape and indicating the location of necessary superstructure; and 6. planes and risers—the short connection between the planes and the fairing—represented by black triangles and short black lines, respectively. As mentioned previously, these illustrations are simplified; they, therefore, lack some functional elements (e.g. a rudder) that would be found on the actual boat.

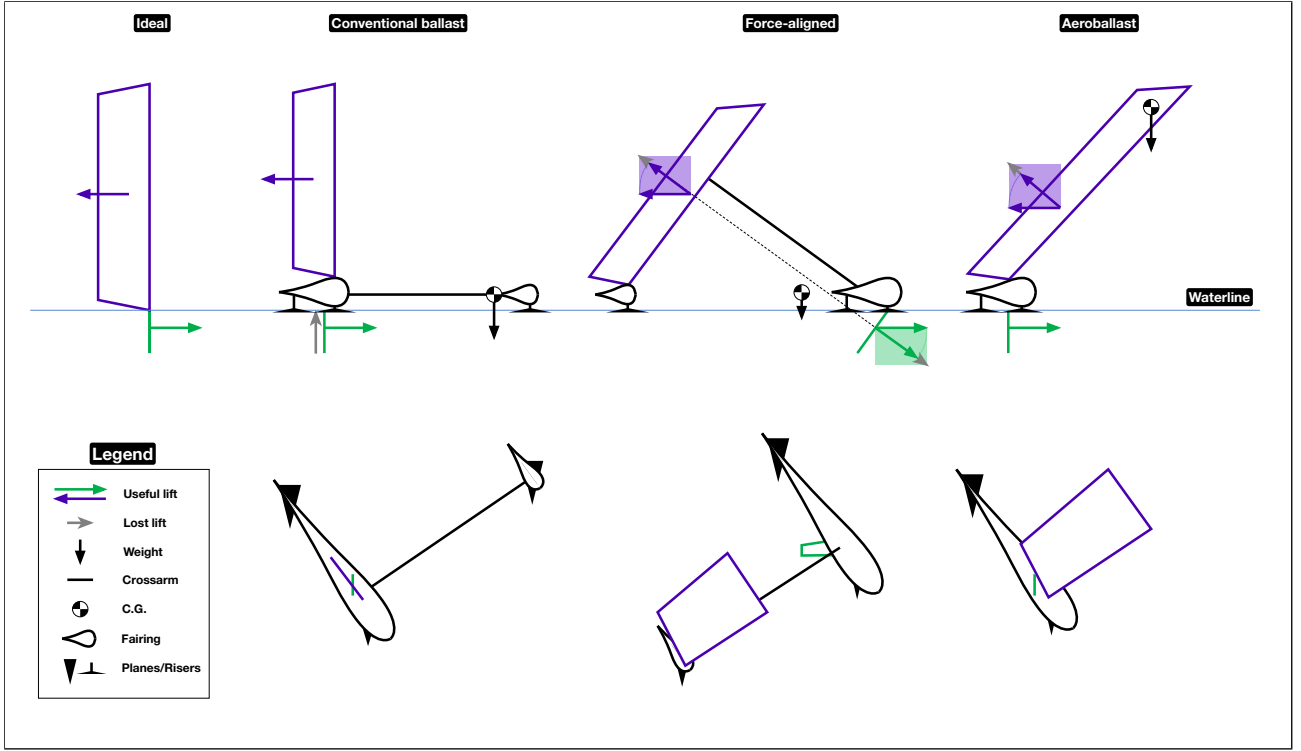


Figure 9: Front and top views of the three primary balancing mechanisms for high-speed sailboats compared alongside an ideal sailboat

What we will come to show is that **aero-hydrodynamic coupling (i.e. the mechanism used to balance the heeling moment) determines the efficiency of real-world (i.e. non-ideal) sailboats**. We will break this down in the next several sections, using those six aforementioned good design assumptions to fairly compare the efficiencies of the three balancing mechanisms in Figure 9.

6. Aero-hydrodynamic coupling determines the efficiency of real-world sailboats and, therefore, their top speed potentials.

3.6.2 Decoupling Lift and Drag

Glide angles proved useful for establishing the quantitative expression for efficiency in Equation 6 because we were able to use the convenient geometric approach presented in Figure 8 (i.e. the Beta Theorem). But in order to move forward with a detailed analysis of the three balancing mechanisms, we actually need to decouple the aerodynamic and hydrodynamic components of lift and drag from the aerodynamic and hydrodynamic glide angles using Equation 1.

The main reason we need to decouple them has to do with the way the three-dimensional components of lift and drag contribute to a loss of efficiency on real-world sailboats. And we will show over the next several sections that this **loss of efficiency is due primarily to two phenomena: 1. the lift that is lost in balancing the heeling moment; and 2. the drag build-up on superstructure**. So while it was handy

for us at the time to couple lift and drag into a single angle in order to quantify efficiency using a geometric approach, we now need to decouple them in order to analyze efficiency losses specific to various balancing mechanisms.

We begin by converting Equation 6 into a form involving L/D , the glide ratio, instead of ε , the glide angle. Recalling Equation 1, we know that $\cot \varepsilon = L/D$. But in Equation 6, we have the sum of two angles, each with a unique L/D . Conveniently, there is a trigonometric identity for the cotangent of the sum of two angles:

$$\cot(\alpha_1 + \alpha_2) = \frac{\cot \alpha_1 \cdot \cot \alpha_2 - 1}{\cot \alpha_1 + \cot \alpha_2} \quad (7)$$

Using this identity, we can transform Equation 6 into

$$\eta = \frac{\cot \varepsilon_A \cdot \cot \varepsilon_H - 1}{\cot \varepsilon_A + \cot \varepsilon_H} \quad (8)$$

And again recalling Equation 1, we can then transform Equation 8 into

$$\eta = \frac{\left(\frac{L}{D}\right)_A \cdot \left(\frac{L}{D}\right)_H - 1}{\left(\frac{L}{D}\right)_A + \left(\frac{L}{D}\right)_H} \quad (9)$$

To highlight the fact that we have decoupled L and D , we can write it like this:

$$\eta = \frac{\frac{L_A}{D_A} \cdot \frac{L_H}{D_H} - 1}{\frac{L_A}{D_A} + \frac{L_H}{D_H}} \quad (10)$$

With some further modification, Equation 10 above is what we will use to compare real-world sailboat efficiencies in Section 4.2.

7. The three-dimensional components of lift and drag contribute to a loss of efficiency on real-world sailboats in primarily two ways: 1. the lift that is lost in balancing the heeling moment; and 2. the drag build-up on superstructure.

3.6.3 Useful Lift and Lost Lift

We previously introduced the concepts of ‘useful’ and ‘lost’ lift in Sections 3.6.1 and 3.5, respectively, and will now qualify these terms. Within the context of high-speed sailing, the comparison to the ideal sailboat turns out to be an apt one because—when you think about it—nothing can go faster than an ideal sailboat. Given a specific wing and foil combination, the ideal sailboat comprising the two will always be faster than any other real-world sailboat comprising the two. It truly defines the upper speed limit of a given sailboat configuration because it directly ties the lift and drag characteristics of the wing and foil to the maximum achievable efficiency, which, again, is the boat speed to true wind speed ratio.

On an ideal sailboat, 100% of the lift produced on the wing and foil is useful because it is all used to propel the sailboat forward. On a real-world sailboat comprising not only a wing and a foil, but also planes, this is not the case. On every real-world configuration, including the aeroballast concept introduced here, there is some amount of lift produced by the wing, planes, and/or foil that is lost in the balancing act. And fortunately for us, it turns out that we can actually quantify this lost lift by analyzing the force and moment vectors acting on a real-world sailboat in all three dimensions.

Before we begin with this detailed quantitative analysis, let us take a qualitative look at the three balancing mechanisms illustrated in Figure 9. The conventional ballast configuration uses windward weight to balance the heeling moment. Its wing and foil are vertical and, therefore, produce no lost lift. However, because it must remain afloat, the planing surfaces must support the entire weight of the sailboat. Therefore, all of the lift produced by the planes is lost lift. The force-aligned configuration uses upward lift on the wing and downward lift on the foil to balance the heeling moment. We assumed zero lift on the planes in our fifth good design assumption from earlier. Therefore, as is illustrated in the diagram, both the wing and the foil [but not the planes] produce lost lift. The aeroballast concept introduced here balances the heeling moment much like a windsurfer. It leans its wing into the wind, using ballast internal to the wing and near the top to remain balanced. The foil remains vertical and so produces no lost lift. Again we assumed its planes produce zero lift. Therefore, as is illustrated in the diagram, only the wing produces lost lift.

The final takeaway from Figure 9 is an important one regarding the useful lift produced by all three configurations. As shown, it is parallel to the waterline and is, therefore, the only lift you see when looking at a top view diagram. In other words, it is exactly the same as L_A and L_H on an ideal sailboat! It is only once we take into account the forces and moments in all three dimensions that the efficiency differences among the balancing mechanisms become apparent. Another way to say this is that **we quantify useful and lost lift by balancing the three-dimensional force and moment equations.**

8. We quantify the useful and lost lift of real-world sailboats by balancing the three-dimensional force and moment equations.

3.6.4 Drag Build-up on Superstructure

In Section 3.6.2, we introduced the concept of ‘drag build-up’ on superstructure and will now qualify exactly what this means. First, superstructure is any aerodynamic element not producing any useful lift. It was even implied in our sixth good design assumption, that superstructure is minimized and streamlined. It is minimized because it does not produce useful lift, and it is streamlined in order to minimize drag.

And when talking about drag in the field of aerodynamics, we commonly use a technique called drag build-up to predict the amount of drag on an aerodynamic device such as an airplane, a device not very different from everything above the waterline on a high-speed sailboat. Stated simply, **the drag build-up technique computes the total drag on an arbitrary shape by adding up the individual drag contributions from each of the known shapes it comprises.** We will not go into this specific technique in rigorous detail, but we will walk through the total drag computations for each of the three balancing mechanisms shown in Figure 9.

9. We quantify the drag build-up on real-world sailboats by adding up the drag contributions from each of the known shapes it comprises.

4 Invention

4.1 Practical Considerations

4.1.1 50 Knot Wall & Supercavitating Foils

At boat speeds approaching 50 knots, the formation of vapor bubbles on the low pressure side of conventional hydrofoils marks the onset of cavitation. And at modern record breaking speeds approaching 70 knots, these small vapor bubbles have combined to form a single cavitation bubble completely enveloping the low pressure side and extending past the trailing edge, as shown in Figure 10. This ‘bubble’ effectively puts the

brakes on even the best conventional racing sailboats equipped with conventional foils such as those seen in the 35th America’s Cup because it reduces the efficiency of conventional foils by about an order of magnitude. The low vapor pressure of water—the pressure throughout the bubble—relative to the high dynamic pressure of water on the lifting side of the foil creates a pronounced increase in the pressure differential across the foil as well as a pronounced rearward tilt of the resultant force vector (i.e. an increase in ϵ).

Supercavitating foils, on the other hand, have a strikingly different shape designed to minimize the drag rise by minimizing the size of the bubble: a sharp leading edge and a blunt trailing edge (or face), causing the bubble to form and, therefore, collapse earlier while also reducing its size in the direction perpendicular to the flow (shown exaggerated as compared to the conventional foil in Figure 10). As a side note, the steep drag rise accompanying the onset of cavitation is why, as shown in Figure 11, the one-of-a-kind boat *Yellow Pages*, a highly optimized yet conventionally ballasted sailboat, held onto a sub-50 knot outright speed record for over a decade starting in the early ’90s, the longest single stretch of time since 1972, when the WSSRC began sanctioning records—more about that in the next section. A handful of windsurfers further increased this record, but this seeming stagnation just below the coincidentally round speed of 50 knots led to talk in the high-speed sailing community—sailors being the superstitious creatures they are—about a magical *50 knot wall*.

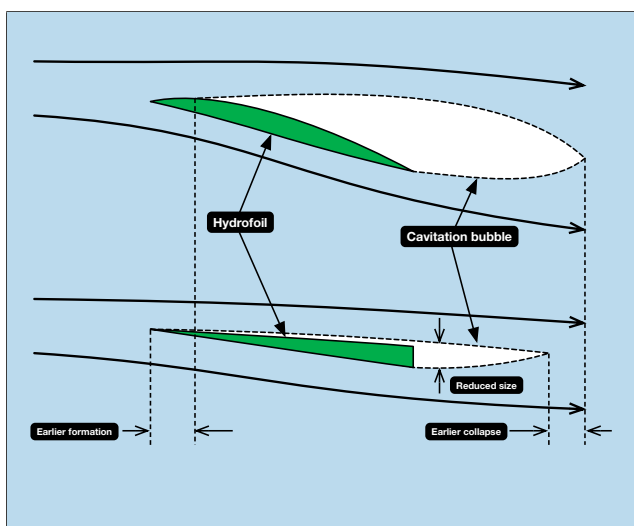


Figure 10: Comparison of conventional (top) and supercavitating (bottom) foil shapes

Finally, in 2008, at an annual speed sailing event in very high winds off the coast of Luderitz, Namibia, a kiteboarder by the name of Sebastien Cattelan set a speed record just above 50 knots, ultimately marking the beginning of the modern high-speed sailing era characterized by supercavitation. It was around this same time that a force-aligned boat named *Sailrocket*, a boat project led by the experienced and charismatic

sailor Paul Larsen, was coming into its own and seeing successes at speeds above 50 knots. These early successes even put them in the record books in the B Class and ultimately inspired the Vestas wind turbine company to sponsor their second boat, *Vestas Sailrocket 2*. Kiteboarders had, in the meantime, continued to push the record upward of 55 knots, but it was this second version of *Sailrocket* that would go on to set the current outright record three times in a row, the latest and fastest being a monumental and inspiring achievement for those of us in the high-speed sailing community. They did not just set a new record, they smashed the old ones by achieving a 500 m average speed of 65.45 knots and a sustained nautical mile average of 55.32 knots! What the kites first demonstrated, and what *Vestas Sailrocket 2* proved beyond a doubt, is that **modern high-speed sailboats can [and must] operate at supercavitating speeds so their foils must be designed with this consideration in mind.**

4.1.2 WSSRC Rules

So far we have made several references to the ‘outright’ sailing speed record, but we have not said anything about how these records are set and sanctioned [or ratified] in the first place. The governing body of the sport of high-speed sailing is actually a relatively new one. It was established in 1972 for the sole purpose of sanctioning sailing records, all the way from the 500 m course record (i.e. the outright record) on the short end up to the round the world non-stop record on the long end. **Its name is the World Sailing Speed Record Council, or WSSRC for short, and its published rules establish the dos and don’ts for the craft itself as well as the timing, officiating, and venue requirements [among others] for record setting attempts.** It is thanks to this governing body that we have a legitimate sport in the first place so perhaps it is a good time to mention that there are additional aspects of Figure 11 worth mentioning which were not immediately relevant to the supercavitation discussion but which are relevant to the sport of high-speed sailing in general. To begin with, it is clear that when looking at all outright records ratified by the WSSRC since 1972, an interesting trend has developed: for a decade or more at a time, a particular type of sailing craft tends to dominate. And so far, there have been three of these distinct eras, all of which are shaded and labeled in Figure 11 [6].

The first of these eras, which is shaded in green and labeled ‘Boats’, was dominated entirely by the *Crossbow* series of conventionally ballasted catamarans. The second era, which is shaded in red (magenta) and labeled ‘Surfers’, began in 1986 when for the first time a windsurfer set the outright speed record, namely at 38.86 knots and just a couple knots higher than the previous record. Windsurfers continued to dominate for the next two decades, with the notable exception

of the aforementioned yacht *Yellow Pages*. The third and current era, which is shaded in purple and labeled ‘Kites’, would mark not only the end of the windsurfer era but also the beginning of speed records in excess of the aforementioned 50 knot wall. This era is labeled Kites because the era began with them, and as we will come to show in Section 4.2.2, both kites and force-aligned boats are analyzed in exactly the same way, the only difference being that the design space for the two is bounded on one end by kites and the other end by fully force-aligned boats. A notable record-setting exception in this modern era of the kites is the foiling trimaran *Hydroptère*, which set an outright record of 51.36 knots in 2009. It is notable not only because it is a conventional ballast configuration but also because it has surface piercing hydrofoils and a flexible sail. It is the most boat-like and seaworthy record setter on the entire graph.

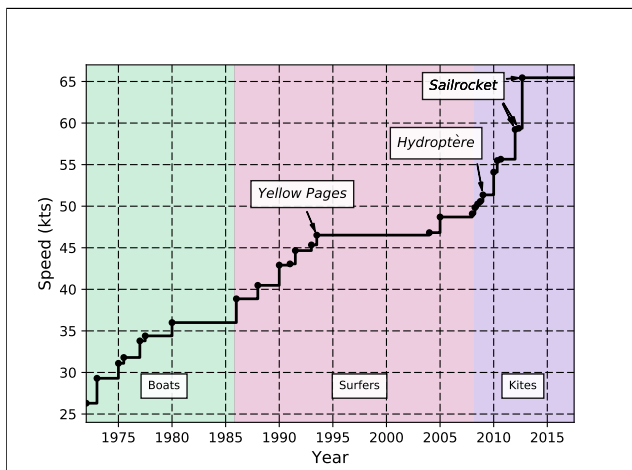


Figure 11: Outright (500 m) sailing speed records as ratified by the WSSRC, which was established in 1972 [6]

Finally, perhaps as important as what is on the graph is what is not there. More specifically, since kiteboarders first managed to set an outright record above 50 knots in 2008, every other type of balancing mechanism has since managed to set records above 50 knots as well. Of particular note is a conventional ballast configuration named *Macquarie Innovation*, which was an improvement on the *Yellow Pages* design [and by the same team] and which we referenced earlier when introducing the different balancing mechanisms in Section 3.6.1. They just barely missed setting the outright record—they do hold a C Class record, however—with a 500 m average of 50.07 knots in 2009 because by that time, the kiteboarders were just a hair faster. And in the ensuing years, windsurfers have continued to raise the bar as well, with their latest Windsurfer class record of 53.27 knots having been set in 2015.

4.1.3 Favorable Aerodynamics

As mentioned in the previous section, the hydrodynamic domain is defined by the necessity to account

for the drag rise that accompanies the onset of cavitation on the foil, about which the information is somewhat limited. On the other hand, the sail and superstructure elements operate entirely within the well understood realm of low-speed aerodynamics, which is another way of saying that the apparent wind speeds are much lower than the speed of sound. The drag on aerodynamic elements is both predictable and, fortunately for us, very efficient. In practice, the efficiencies of wings at the apparent wind speeds necessary for record breaking are an order of magnitude better than the efficiencies of supercavitating foils at these same record breaking speeds. What this means, then, is that as sailboat designers, we are better off trading hydrodynamic losses for aerodynamic ones. To say it another way, **we would rather pay an aerodynamic penalty than a hydrodynamic one so we need to optimize aerodynamics as much as possible.**

4.1.4 Seaworthiness & Absolute Speed

Up to this point, we have spent a good bit of time establishing that efficiency is what we use to compare top speed potentials. Although this allows us to determine how well a design performs in a relative sense, it is not enough to tell us how a design performs in an absolute sense. In order to do this, we must take a step back, to Section 3.4, and recall the first of our two intuitive assumptions about hypothetical sailboats A and B: ‘If A and B are identical, but A is sailing in higher true winds than B, A will sail faster than B.’ At the time, we focused on the second assumption regarding efficiency because it was what we needed for establishing our comparison framework. But it is this first assumption which must be a practical consideration for any real-world design. What it says, in short, is that in order to go faster than any existing sailboat (i.e. to set a record), **it is not merely enough for a design to be more efficient, it must also be seaworthy in wind conditions high enough to reach record speeds.**

This design consideration becomes even more apparent when taking into account the conditions in which the most recent record setting runs took place. *Vestas Sailrocket 2* set the current record in approximately 28 knots of wind, and the previous record holders, the kiteboarders, set their records in even higher winds ranging from 40 to 50 knots. What is noteworthy about these wind speeds is that in open water the corresponding wave height would be anywhere from 15 - 30 feet high. Suffice it to say, the aforementioned record setters did not operate in open water. Instead, they each found their own special location with regularly high winds blowing off of a beach into protected waters, where the wave height, instead of being elevated by the wind, is limited by the fetch, the distance wind travels over the water to your boat, to the small ripples seen in a pool on windy days.

These special conditions are both rare and difficult to work with from a record setting point of view. They strain even the best laid time, travel, and support plans, while at the same time making it nearly impossible to gather the valuable sailing experience necessary to make a record setting sailboat truly worthwhile in a practical sense. It also precludes the ability to use these same sailboats for offshore records [as they are designed for these special conditions]. So in order to build the next record setting high-speed sailboat, and one with the ability to sail fast in both offshore as well as coastal waters, the seaworthiness of modern high-speed sailboats is an imperative consideration.

On a somewhat related sidenote, we sailors conventionally think in terms of powering up to go faster, that a greater sail area will result in greater power and, therefore, faster speeds. This legacy thinking is inspired by the tradition of sailing heavy keelboats, which historically have been underpowered and inefficient. And, intuitively, it would seem to make sense that the resistance of the water, which we know from experience to be much higher than that of air, is what limits our speed. Although intuition and legacy thinking serve us well as sailors in practice, they are extraneous considerations when compared against the insights provided by the Beta Theorem for the design of high-speed sailboats, which highlight the relationship of top speed potential to efficiency, not power.

4.1.5 Fastest Point of Sail & η_{max}

While establishing our theoretical framework in Section 3, we alluded to an important point requiring further discussion: fastest point of sail in Section 3.4. Although it was not of direct consequence for establishing the efficiency relationships required for comparing the top speed potentials of high-speed sailboat designs, it did serve as a jumping-off point for this final practical consideration. Recalling Figure 8, we arranged the true wind and hydrodynamic velocity vectors perpendicularly in order to establish the convenient relationship between η and β in Equation 4. And it was this arrangement which ultimately enabled us to derive [using the Beta Theorem] the relationship between η , $(L/D)_A$, and $(L/D)_H$ in Equation 10, which is what we will use in the next section for an efficiency comparison.

But in order to maximize efficiency in an absolute sense, we must take a second look at the diagram in Figure 8. **By reorienting the true wind vector, V_T , so that it is now perpendicular to the apparent wind vector, V_A , as shown in Figure 12, we have maximized efficiency.** The new trigonometric relationship for maximum efficiency, η_{max} , is then

$$\eta_{max} = \csc \beta \quad (11)$$

And η_{max} is related to our η from the previous sections by the simple relationship

$$\eta_{max} = \sqrt{\eta^2 + 1} \quad (12)$$

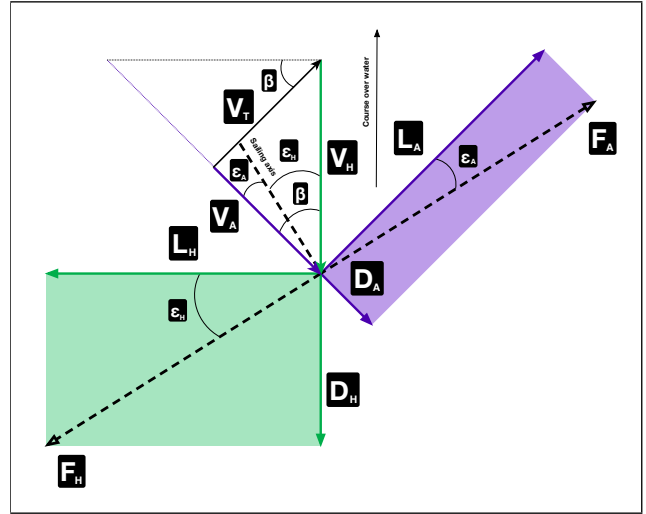


Figure 12: Modified version of Figure 8 illustrating the relationship of β to the fastest point of sail

10. There are five practical considerations for speed record attempts: 1. Supercavitating Foils; 2. WSSRC Rules; 3. Favorable Aerodynamics; 4. Seaworthiness; and 5. Maximum Efficiency.

4.2 Efficiency Comparison

This efficiency comparison is of a technical nature, applying knowledge from undergraduate level courses in Aerodynamics and Statics to quantify and, therefore, compare efficiencies for the three high-speed sailboat configurations illustrated in Figure 9. New ideas are introduced with less qualification than in the previous sections, which were more narrative rather than technical.

For analysis purposes, we further simplified the force arrangement among the aerodynamic, hydrodynamic, and weight vectors down to the free body diagrams shown in Figure 13, each of which is a front view from a point along the sailing axis. The purple and green convention is again used to indicate aerodynamic and hydrodynamic resultant force vectors, respectively. The structure is all but removed and replaced instead with dashed lines. The arrangement of the forces is idealized in order to simplify the analysis. For example, the conventional ballast configuration has a single hydrodynamic resultant force vector pointing upward at an angle ϕ_H , but in reality, this single resultant force would likely be the result of upward forces on three planes and a windward force on a foil. And the force-aligned configuration has a colocated C.G. and hydrodynamic resultant force vector, which greatly simplifies the analysis by allowing the sum of the hydrodynamic and weight forces to be analyzed together in the force balance equations.

We have to refine our efficiency equation a bit more in order to move forward. Recalling Equation 10 for efficiency in terms of the decoupled aerodynamic and hydrodynamic lift and drag components, we know that

$$\eta = \frac{\frac{L_A}{D_A} \cdot \frac{L_H}{D_H} - 1}{\frac{L_A}{D_A} + \frac{L_H}{D_H}} \quad (13)$$

But these lift and drag components are only those components of the aerodynamic and hydrodynamic forces parallel to the waterline plane. It is what we earlier called the useful lift. Taking a moment to consider the possible orientations of the two lift-producing elements, the wing and the foil, on a real-world sailboat, we realize that each can be rotated by some angle ϕ relative to the relevant fluid (i.e. air or water) direction. In other words,

$$L_A = L_w \cdot \cos \phi_w \quad (14)$$

and

$$L_H = L_f \cdot \cos \phi_f \quad (15)$$

Using the drag build-up technique, we can compute the total aerodynamic drag D_A by adding up the individual drag contributions from N constituent aerodynamic regions of the overall structure in addition to the wing. So we can say that

$$D_A = D_w + D_1 + D_2 + \dots + D_N = D_w \cdot k_D \quad (16)$$

As shown above, the total aerodynamic drag D_A can be reduced down to a single scaling factor k_D multiplied by the drag on the wing, D_w , a simplification that comes in handy for manipulating Equation 13 into a more useful form.

Hydrodynamic drag, D_H , is assumed equal to the foil drag, D_f , as we would rather pay an aerodynamic penalty than a hydrodynamic one and, therefore, reduce the waterborne structure down to a single foil for analysis purposes. Therefore,

$$D_H = D_f \quad (17)$$

For completeness, it is important to note that the wing and foil have the following associated glide angles:

$$\varepsilon_w = \cot^{-1} \left(\frac{L}{D} \right)_w \quad (18)$$

and

$$\varepsilon_f = \cot^{-1} \left(\frac{L}{D} \right)_f \quad (19)$$

By substituting Equations 14, 15, 16, and 17 into Equation 13 and simplifying, we have

$$\eta = \frac{\left(\frac{L}{D} \right)_w \cdot \frac{\cos \phi_w}{k_D} \cdot \left(\frac{L}{D} \right)_f \cdot \cos \phi_f - 1}{\left(\frac{L}{D} \right)_w \cdot \frac{\cos \phi_w}{k_D} + \left(\frac{L}{D} \right)_f \cdot \cos \phi_f} \quad (20)$$

This expression is the one we will use for our comparison, and it turns out to be a convenient one because three of the terms, namely ϕ_w , ϕ_f , and k_D , are dependent variables of a single independent design variable k_l . So, really, we have an efficiency expression dependent on the efficiency of the wing as represented by its glide ratio $(L/D)_w$, the efficiency of the foil as represented by its glide ratio $(L/D)_f$, and a single design variable k_l . So what exactly is this design variable k_l ? It takes on a slightly different meaning for each of the three configurations so an appropriate description will accompany each analysis to follow.

We will now move forward with this comparison by balancing the three-dimensional force and moment equations and computing the drag build-up for each of the three balancing mechanisms. As stated previously, each of the three free body diagrams in Figure 13 is a front view from a point along the sailing axis, indicated by the dashed line dividing β in Figures 8 and 12. We call this the sailing axis because it can be thought of as an unbiased sailing direction of sorts. After all, a sailboat is moving through both the water *and* the air. Without belaboring this somewhat philosophical point, suffice it to say that we traditionally think in terms of a sailboat moving over the water because, historically, this is nearly the same as moving over the ground, which was the practical impetus for the nautical tradition (e.g. trade, migration, etc.).

By aligning our coordinate system with this sailing axis, which is perpendicular to the aerodynamic and hydrodynamic resultant force vectors, F_A and F_H , the number of force and moment equations is reduced by a factor of two from six to three. Whereas we previously depicted these mechanisms graphically in Figure 9 to develop a mental picture of the physical (or structural) arrangement, we are now illustrating them without any graphical elements in a greatly simplified manner in order to emphasize the simple elegance of the force and moment relationships.

Up to this point, we have been somewhat loose in our notation concerning vectors. To clarify, the resultant force and weight vectors actually take the following form:

$$\vec{F}_A = -F_{A_y} \hat{j} \pm F_{A_z} \hat{k} \quad (21)$$

$$\vec{F}_H = F_{H_y} \hat{j} \pm F_{H_z} \hat{k} \quad (22)$$

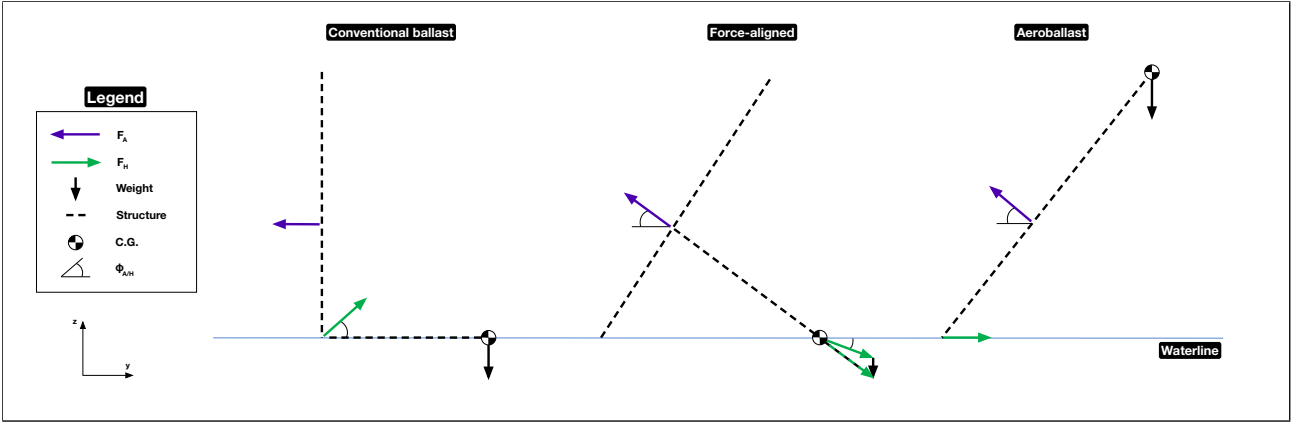


Figure 13: **Front views of the three primary balancing mechanisms as seen from a point along the sailing axis, which is perpendicular to the aerodynamic and hydrodynamic resultant force vectors**

$$\vec{W} = -W\hat{k} \quad (23)$$

In the succeeding sections we will drop the \hat{j} and \hat{k} unit vectors as they are implied.

Finally, from Figure 13, we can see that the horizontal components of the aerodynamic and hydrodynamic resultant force vectors must always be equal and opposite for all configurations. Therefore,

$$F_{A_y} = F_{H_y} \quad (24)$$

This equivalence means that the number of unique equations to analyze for each configuration drops even further from three down to two.

For the drag build-up, we are using the dimensions of *Vestas Sailrocket 2* as a baseline for comparison purposes as it is obviously a well-designed boat and is nearly a one-to-one match with the outline drawing of a force-aligned sailboat shown in Figure 9. By doing a photogrammetry analysis of available design images, we are able to estimate the various cross sectional and planform areas of the structural regions on the boat [7]. We care about four regions in particular, namely the fuselage [with risers below it connected to hulls], hulls, pod, and crossarm. These four superstructure regions are each referenced to the drag on the wing by a scaling factor k_D . Some of these scaling factors scale with k_l or even k_l^2 depending on the boat and the design assumptions used. For shapes such as the fuselage, pod, and hulls, we are using a C_D of 0.04 referenced to their cross-sectional areas. And for shapes such as the crossarm and risers, which connect the hulls to the fuselage, we are using a C_D of 0.01 referenced to their planform areas. For simplification, the scaling factor for the fuselage includes the total drag from two risers in addition to the fuselage. And the scaling factor for the pod includes the total drag from one riser, one hull, and one streamlined body half the diameter of the fuselage.

4.2.1 Conventional Ballast

The conventional ballast configuration has a crossarm connecting the windward pod to the fuselage, atop which the wing is mounted vertically. The fuselage and pod are aligned with the apparent wind direction while the crossarm, which is horizontal, is perpendicular to it. Figure 14 is what we would see if we were looking at just the superstructure [not including the risers and hulls] from a point upwind.

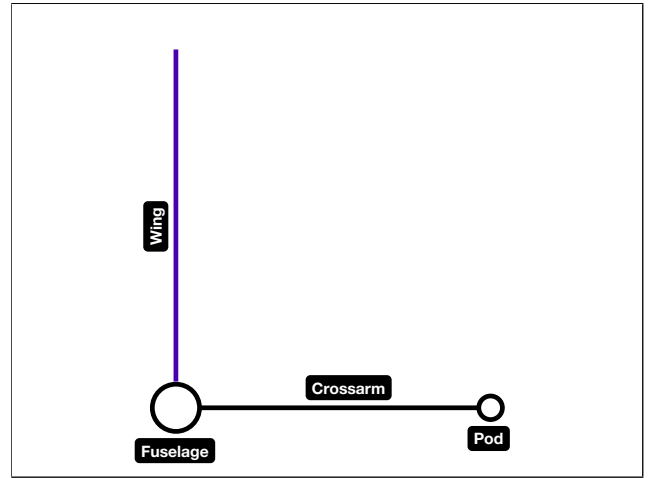


Figure 14: **Superstructure of the conventional ballast configuration, not including the risers and hulls, as viewed from a point upwind**

We define a design variable k_l as the ratio of the crossarm length to the spanwise location of the aerodynamic center of the wing. Therefore,

$$k_l = \frac{l_{crossarm}}{b_{ac}} \quad (25)$$

By design, the wing on the conventional ballast configuration is vertical, which means that

$$\phi_w = 0 \quad (26)$$

and, therefore, that

$$F_{A_z} = 0 \quad (27)$$

The vertical force balance equation, therefore, is simply

$$W = F_{H_z} \quad (28)$$

Moving onto the moment balance equation by choosing a point at the origin of the green vector in Figure 13 and summing the moments about the apparent wind vector, we have

$$L_w - W \cdot k_l = 0 \quad (29)$$

We know L_w is related to F_{A_y} by the trigonometric relationship

$$L_w = F_{A_y} \cdot \cos \varepsilon_w \quad (30)$$

Substituting Equations 28, 24, and 30 into Equation 29 and simplifying, we obtain

$$k_l \cdot \sec \varepsilon_w = \frac{F_{H_y}}{F_{H_z}} \quad (31)$$

Using trigonometry, we can say that

$$\phi_H = \cot^{-1}(k_l \cdot \sec \varepsilon_w) \quad (32)$$

ϕ_H above is the roll angle of F_H and is related to the roll angle of the foil, ϕ_f , by the trigonometric relationship

$$\phi_f = \sin^{-1}(\sin \phi_H \cdot \sec \varepsilon_f) \quad (33)$$

Moving onto the drag build-up, we can say that the fuselage drag scales linearly with k_l in order to maintain directional authority as the boat widens with k_l . Therefore,

$$k_{D_{fuselage}} = 0.013 \cdot k_l \quad (34)$$

The aerodynamic drag on the hulls is assumed fixed as follows

$$k_{D_{hulls}} = 0.051 \quad (35)$$

The aerodynamic drag on the windward pod is assumed fixed as follows

$$k_{D_{pod}} = 0.032 \quad (36)$$

We can now use two different approaches for scaling the aerodynamic drag on the crossarm. We can be pessimistic and assume that the crossarm area scales with k_l^2 , which would be the case for a rigid connection

between the fuselage and the wing. Then the resulting scaling factor is

$$k_{D_{crossarm}} = 0.022 \cdot k_l^2 \quad (37)$$

Or we can be optimistic and assume that the crossarm area scales with k_l , which would be the case for a more kite-like connection between the fuselage and the wing. Then the resulting scaling factor is

$$k_{D_{crossarm}} = 0.038 \cdot k_l \quad (38)$$

For the pessimistic and optimistic crossarm scaling factors above, the resulting k_D values are, respectively,

$$k_D = 1.083 + 0.013 \cdot k_l + 0.022 \cdot k_l^2 \quad (39)$$

and

$$k_D = 1.083 + 0.051 \cdot k_l \quad (40)$$

We now have all we need to compute the efficiency of the conventional ballast configuration using Equation 20.

4.2.2 Force-Aligned [and Kites]

The force-aligned configuration is somewhat similar to the conventional ballast configuration because it comprises an identical set of aerodynamic regions. It has a crossarm connecting the fuselage to the wing, below which is mounted a pod. The fuselage and pod are again aligned with the apparent wind direction while the crossarm is perpendicular to it. The crossarm meets the wing at a right angle, only this time the wing is not vertical. Figure 15 is what we would see if we were looking at just the superstructure [not including the risers and hulls] from a point upwind.

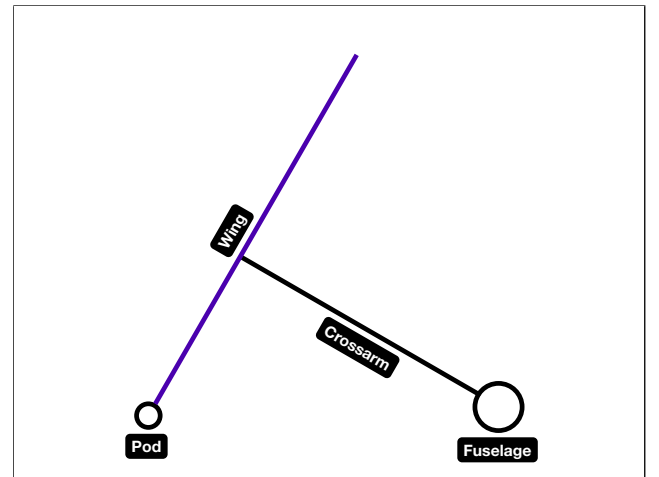


Figure 15: **Superstructure of the force-aligned configuration, not including the risers and hulls, as viewed from a point upwind**

We again define a design variable k_l as the ratio of the crossarm length to the spanwise location of the aerodynamic center of the wing. Therefore,

$$k_l = \frac{l_{crossarm}}{b_{ac}} \quad (41)$$

For the force-aligned concept, there is actually a second unique design consideration in addition to k_l . If we look at Figure 13, we can see that the weight and the downward component of hydrodynamic lift add up to create a net downward force which is in balance with the upward force component of aerodynamic lift. The designer can, therefore, adjust the ratio of downward hydrodynamic lift to weight. A force-aligned boat with no downward hydrodynamic lift—as hinted at in the title of this section—is actually what we would call a kite! To account for this design choice, we define a ballast scaling factor k_b as the ratio of weight to the net downward force as follows

$$k_b = \frac{W}{W + F_{H_z}} \quad (42)$$

The force and moment balance equations for the force-aligned case are actually rather elegant in their simplicity because a force balance is assumed. Therefore, we can proceed directly with relating our dependent variables ϕ_w and ϕ_f to our independent design variable k_l .

By design, we have a crossarm in the aerodynamic domain oriented perpendicularly to the wing and the apparent wind direction. Therefore,

$$\phi_w = \cot^{-1} k_l \quad (43)$$

Assuming a net force alignment, ϕ_f is related to ϕ_w and k_b by the trigonometric relationship

$$\phi_f = \tan^{-1}((1 - k_b) \cdot \tan \phi_w) \quad (44)$$

The drag build-up is the same for the force-aligned configuration as it was for the aforementioned conventional ballast configuration because, as previously mentioned, they share an identical set of aerodynamic regions. Therefore, the same pessimistic and optimistic k_D values apply as follows:

$$k_D = 1.083 + 0.013 \cdot k_l + 0.022 \cdot k_l^2 \quad (45)$$

and

$$k_D = 1.083 + 0.051 \cdot k_l \quad (46)$$

We now have all we need to compute the efficiency of the force-aligned configuration using Equation 20.

4.2.3 Aeroballast

The aeroballast configuration does not have a crossarm or pod like the other two configurations. The fuselage is similarly aligned with the apparent wind direction, and the wing is rotatably mounted to it allowing for the roll angle to be adjusted [and then locked in place]. Figure 16 is what we would see if we were looking at just the superstructure [not including the risers and hulls] from a point upwind.

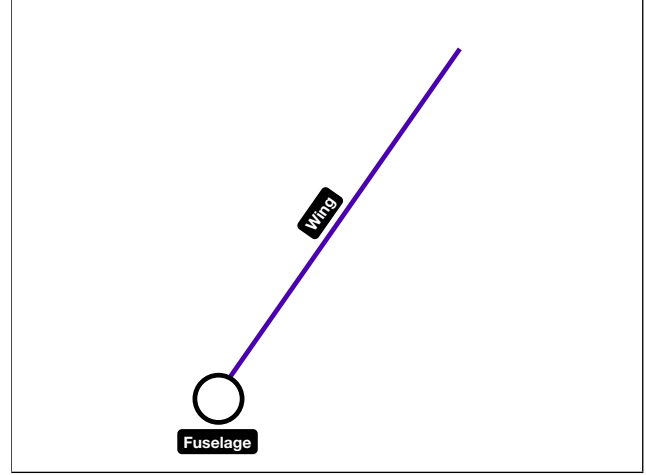


Figure 16: **Superstructure of the aeroballast configuration, not including the risers and hulls, as viewed from a point upwind**

We define a design variable k_l as the ratio of the span of the wing—the tip is where the C.G. is located in the idealized free body diagrams in Figure 13—to the spanwise location of the aerodynamic center of the wing. Therefore,

$$k_l = \frac{b_{wing}}{b_{ac}} \quad (47)$$

By design, the foil is vertical, which means that

$$\phi_f = 0 \quad (48)$$

and, therefore, that

$$F_{H_z} = 0 \quad (49)$$

The vertical force balance equation, therefore, is simply

$$F_{A_z} = W \quad (50)$$

By definition, L_A and D_A are parallel to the waterline plane. We can, therefore, relate F_{A_z} —which is perpendicular to it—to L_w and ϕ_w with the following relationship:

$$F_{A_z} = L_w \cdot \sin \phi_w \quad (51)$$

Substituting Equation 50 into Equation 51, we obtain

$$W = L_w \cdot \sin \phi_w \quad (52)$$

Moving onto the moment balance equation by choosing a point at the base of the wing in Figure 13 and summing the moments about the apparent wind vector, we have

$$L_w - W \cdot k_l \cdot \sin \phi_w = 0 \quad (53)$$

By substituting Equation 52 into 53, we obtain

$$\phi_w = \csc^{-1} \sqrt{k_l} \quad (54)$$

The drag build-up for the aeroballast configuration is significantly different from the previous two configurations. There is no crossarm or pod. The fuselage drag scaling factor, $k_{D_{fuselage}}$, does not scale with k_l because the boat does not widen as k_l increases. It is, therefore, a constant as follows:

$$k_{D_{fuselage}} = 0.022 \quad (55)$$

The drag scaling factor for the hulls, $k_{D_{hulls}}$, remains the same as it did for the conventional ballast configuration, which was given in Equation 35. Therefore, the new k_D value, which is the sum of 1 and these two constants $k_{D_{fuselage}}$ and $k_{D_{hulls}}$, is also a constant as follows:

$$k_D = 1.073 \quad (56)$$

We now have all we need to compute the efficiency of the aeroballast configuration using Equation 20.

4.2.4 Results

In order to complete the efficiency comparison, we must assume values for $(L/D)_w$ and $(L/D)_f$ for inclusion into Equation 20, which up until this point we have ignored. Reasonable values for these properties are 40 and 3, respectively. As expected, there is an order of magnitude difference in the two values, which we went over in Section 4.1.3. The latter value, for $(L/D)_f$, is a value based on the performance of *Vestas Sailrocket 2*, which we again use here for comparison because it is well designed and is the only working example of a sailboat with a supercavitating foil, which is a requirement at current record speeds [7].

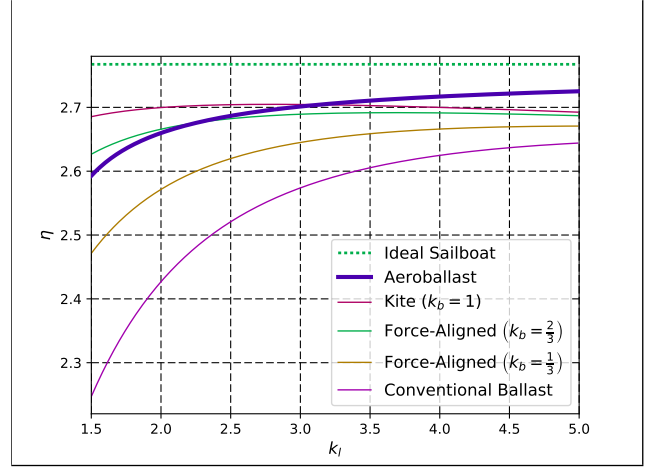


Figure 17: **Efficiency comparison using an optimistic aerodynamic drag build-up for the crossarms on the conventional ballast and force-aligned configurations**

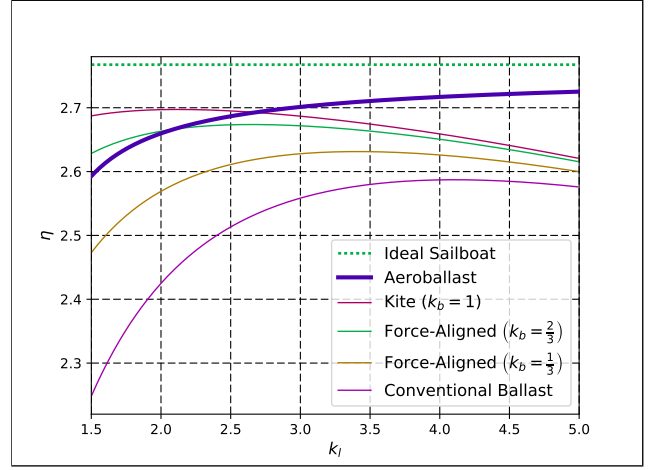


Figure 18: **Efficiency comparison using a pessimistic aerodynamic drag build-up for the crossarms on the conventional ballast and force-aligned configurations**

Efficiency values were calculated for five configurations: 1. conventional ballast; 2. force-aligned where $k_b = 1/3$; 3. force-aligned where $k_b = 2/3$; 4. force-aligned [or kite] where $k_b = 1$; and 5. aeroballast. Their efficiencies were calculated across a k_l range of 1.5 - 5 using both the optimistic and pessimistic drag build-up assumptions, which apply specifically to the crossarms for the conventional ballast and force-aligned configurations only and which are plotted separately in Figures 17 and 18, respectively.

The dashed line labeled ideal sailboat is the upper bound one could expect for the assumed $(L/D)_w$ and $(L/D)_f$ values and was computed by substituting these two values in for $(L/D)_A$ and $(L/D)_H$, respectively, into Equation 9. A comparison of the two graphs illustrates the sensitivity of the conventional ballast and force-aligned configurations to the assumptions about drag on their crossarms. And in both cases, there is a diminishing return as k_l is increased beyond a certain point, which is unique for each configuration. On the other hand, **the efficiency of the aeroballast configura-**

tion continues to grow as k_l increases, and for $k_l > \sim 3.5$, its efficiency exceeds the maximum efficiency of all other configurations.

Of further interest is what these graphs tell us about force-aligned boats: the most efficient variation is the kite version, which has a k_b value of 1. Intuitively, this makes sense because the foil is vertical in this case [because there is no downward lift on it] thereby minimizing lost lift in the relatively inefficient hydrodynamic domain. Another interesting realization is what a pronounced impact the choice of k_b has on maximum efficiency. The lower the value of k_b , the lower the value of maximum efficiency.

Considering further the kite variation, its maximum efficiency occurs at a k_l value anywhere from 2.25 - 2.75, depending on the crossarm drag assumptions used. In practice, kites have much higher k_l values closer to 10, at which point the efficiency is far below its maximum. So what this data suggests is that for faster speeds, the kiteboarders should actually shorten their connections and perhaps add weight to their boards to account for the increased upward lift resulting from the corresponding ϕ_w increase.

A reasonable question at this point is where *Vestas Sailrocket 2* falls within the k_b spectrum. Based on the available data from their website, their boat has a value of k_l , as defined in Equation 41, equal to about 1.4. And during their record run, they sailed at a boat speed to wind speed ratio of around 2.4 [7]. Assuming this value is equal to η_{max} from Equation 12, the corresponding value for η —this is what is plotted in Figures 17 and 18—would be about 2.2. Although its k_l value falls outside of our analysis range, suffice it to say that its k_b value would be at or close to 0, as expected. But this is only an estimate as we have idealized the configurations in Figure 13 for this analysis, not to mention made several drag build-up and good design assumptions that differ from the real-world configuration of their boat in non-trivial ways.

11. Aeroballast has the highest maximum efficiency of the three design configurations, the next highest being the kite variation of the force-aligned configuration.

4.3 Sailing Aeroballast in Practice

We have devoted almost this entire paper to the efficiency comparison, but now we will discuss how aeroballast is sailed in practice. Because it has a C.G. above the waterline, it is statically unstable. It must, therefore, have a well-designed control system to enable the sailor to actively keep the boat upright much like a windsurfer does. This is one of the first test objectives for an approximately $1/10^{\text{th}}$ scale radio control research model currently under construction. Although not trivial, this can be done.

Additional practical benefits of the aeroballast config-

uration are **enhanced seaworthiness and tackability**. It has a more compact superstructure, meaning primarily that it lacks exposed regions like the crossarms on the other two configurations. These exposed regions pose both a directional authority challenge as well as a slamming challenge in higher sea states. The aeroballast configuration can, therefore, withstand higher sea states making it offshore capable. And in order to tack, it turns its hulls and adjusts the roll angle of the wing, enabling it to be raced in a conventional way. **It is not merely meant to set records; it is meant to be sailed in a practical sense for recreation and competition.**

12. Aeroballast can be tacked and sailed in higher sea states than other high-speed sailboat configurations and is meant to be used for recreation and competition.

4.4 The Speed Limit of Sailing

We started out in our very first roadmap entry by asking the fundamental question of sailing: How fast can a sailboat go?

It turns out that we already have everything we need to answer that question. We know that a sailboat's top speed is determined by first calculating η from Equation 20 and then calculating η_{max} from Equation 12. The next step is then a relatively straightforward one: simply multiply that η_{max} value by the maximum wind [and sea] conditions in which a given configuration can sail. If we choose the hypothetical aeroballast configuration from Section 4.2.4, which has $(L/D)_w$, $(L/D)_f$, and k_l values of 40, 3, and 3.5, respectively, then our maximum theoretical boat speed to wind speed ratio is 2.89 (the 2.71 value from Figures 17 and 18 is η , not η_{max}). For a range of wind conditions from 20 - 50 knots, the corresponding maximum theoretical boat speed would vary linearly with the wind speed from 58 - 144 knots. In order to match the current record of 65.45 knots, this hypothetical aeroballast configuration would need to sail in 23 knots of wind. And **if sailed in the same 28 knot wind conditions as the current record holder, an aeroballast configuration could theoretically achieve a speed of 81 knots.**

But simply multiplying two numbers together does not bring with it the necessary level of practical experience and confidence necessary to undertake such bold record runs with reckless abandon, so to speak. The lesson we all learned from *Vestas Sailrocket 2* is that supercavitating sailboats are a reality but also that with any new design, there is a lot of testing that goes along with expanding the sailing envelope into new speed regimes.

13. An aeroballast configuration of closely matched dimensions to the current record holder, Vestas Sailrocket 2, could theoretically achieve a boat speed of 81 knots in the same wind conditions.

References

- [1] Dan McCosh. "Race Around the World: Anything Goes." *Popular Science* Jan. 2001: 62–67, Print.
- [2] Jason Daley. "The Race to 50 Knots." *Popular Science* Oct. 2005: 62–68, Print.
- [3] John Rousmaniere *Annapolis Book of Seamanship*. Simon & Schuster, New York, 1999.
- [4] C. A. Marchaj. *Aero-Hydrodynamics of Sailing*. Dodd, Mead & Company, New York, 1979.
- [5] Ross Garrett. *The Symmetry of Sailing: The Physics of Sailing for Yachtsmen*. Adlard Coles Ltd, London, 1987 (pp. 67–68).
- [6] World Sailing Speed Record Council, <http://www.sailspeedrecords.com>
- [7] Sailrocket, <http://www.sailrocket.com>